Presurgical accuracy of dipole clustering in MRI-negative pediatric patients with epilepsy: Validation against intracranial EEG and resection

Georgios Ntolkeras [a,b,c], Eleonora Tamilia [a,b], Michel AlHilani [a,b,d], Jeffrey Bolton [e], P. Ellen Grant [b,f], Sanjay P. Prabhu [f], Joseph R. Madsen [g], Steven M. Stufflebeam [h], Phillip L. Pearl [e], Christos Papadelis [a,i,j,k,∗]

[a] Laboratory of Children's Brain Dynamics, Division of Newborn Medicine, Department of Medicine, Boston Children's Hospital, Harvard Medical School, Boston, MA, USA
[b] Fetal-Neonatal Neuroimaging and Developmental Science Center, Division of Newborn Medicine, Department of Medicine, Boston Children's Hospital, Harvard Medical School, Boston, MA, USA
[c] Athinoula A. Martinos Center for Biomedical Imaging, Massachusetts General Hospital, Harvard Medical School, Boston, MA, USA
[d] The Hillingdon Hospital NHS Foundation Trust, London, United Kingdom
[e] Division of Epilepsy and Clinical Neurophysiology, Department of Neurology, Boston Children's Hospital, Harvard Medical School, Boston, MA, USA
[f] Division of Neuroradiology, Department of Radiology, Boston Children's Hospital, Harvard Medical School, MA, USA
[g] Division of Epilepsy Surgery, Department of Neurosurgery, Boston Children's Hospital, Harvard Medical School, Boston, MA, USA
[h] Athinoula A. Martinos Center for Biomedical Imaging, Massachusetts General Hospital, Harvard Medical School, Boston, MA, USA
[i] Jane and John Justin Neurosciences Center, Cook Children's Health Care System, Fort Worth, TX, USA
[j] School of Medicine, Texas Christian University and University of North Texas Health Science Center, Fort Worth, TX, USA
[k] Department of Bioengineering, University of Texas at Arlington, Arlington, TX, USA

ARTICLE INFO

HIGHLIGHTS

- Interictal magnetic and electric source imaging (MSI and ESI) using dipole clustering helps localizing the seizure onset zone (SOZ) and irritative zone (IZ) in MRI-negative patients with drug resistant epilepsy (DRE).
- Interictal MSI and ESI using dipole clustering facilitate the prognostic assessment of MRI-negative patients with DRE.
- Clustered dipoles show higher precision to the SOZ and IZ than scattered in MRI-negative patients with DRE.

ABSTRACT

Objective: To assess the utility of interictal magnetic and electric source imaging (MSI and ESI) using dipole clustering in magnetic resonance imaging (MRI)-negative patients with drug resistant epilepsy (DRE).
Methods: We localized spikes in low-density (LD-EEG) and high-density (HD-EEG) electroencephalography as well as magnetoencephalography (MEG) recordings using dipoles from 11 pediatric patients. We computed each dipole's level of clustering and used it to discriminate between clustered and scattered dipoles. For each dipole, we computed the distance from seizure onset zone (SOZ) and irritative zone (IZ) defined by intracranial EEG. Finally, we assessed whether dipoles proximity to resection was predictive of outcome.
Results: LD-EEG had lower clusterness compared to HD-EEG and MEG ($p < 0.05$). For all modalities, clustered dipoles showed higher proximity to SOZ and IZ than scattered ($p < 0.001$). Resection percentage was higher in optimal vs. suboptimal outcome patients ($p < 0.001$); their proximity to resection was correlated to outcome ($p < 0.001$). No difference in resection percentage was seen for scattered dipoles between groups.
Conclusion: MSI and ESI dipole clustering helps to localize the SOZ and IZ and facilitate the prognostic assessment of MRI-negative patients with DRE.
Significance: Assessing the MSI and ESI clustering allows recognizing epileptogenic areas whose removal is associated with optimal outcome.

∗ Corresponding author at: 1500 Cooper St., Fort Worth, TX 76104, USA.
   E-mail address: christos.papadelis@cookchildrens.org (C. Papadelis).

1. Introduction

Up to one third of children with epilepsy develop drug resistance and need neurosurgery to control their seizures (Kwan and Brodie, 2002). Magnetic Resonance Imaging (MRI) can indicate an anatomical lesion related to epilepsy in almost two thirds of all cases and is considered a reliable guide for the definition of the epileptogenic zone (EZ) and the placement of intracranial coverage for localizing the seizure onset zone (SOZ) (McGonigal et al., 2007, Semah et al., 1998). Surgical resection of this lesion is associated with better surgical prognosis (Tonini et al., 2004) and improved seizure control (Berkovic et al., 1995, Radhakrishnan et al., 1998). The remaining patients, in whom the MRI results are inconclusive (i.e. normal or non-focal), are often considered not good surgical candidates. Thus, they are less likely to be offered surgical treatment (Siegel et al., 2001, Tonini et al., 2004).

In patients with inconclusive MRI findings, detailed analysis of ictal and interictal electrophysiology and its correlation with clinical findings is used to guide surgical planning. Electrophysiological methods can be fundamental in these cases since they can point out pathological areas, which may be overlooked on MRI. For example, in about 40% of patients with inconclusive MRI results, surgical biopsies have showed cortical dysplasias (McGonigal et al., 2007). Hence, when MRI is inconclusive, surgical planning depends primarily upon the ability to record clinical seizures and trace the SOZ since this represents the most logical means to estimate the EZ.

The gold standard for delineating the SOZ is by using intracranial electroencephalography (icEEG), with stereo EEG or subdural grids and strips. Yet, icEEG carries significant risks associated with its invasiveness (e.g. infection, bleeding and/or neurological damage) (Hader et al., 2013, Nagahama et al., 2018, Önal et al., 2003). In addition, seizures are unpredictable; thus, long-term monitoring (LTM) of several days (up to weeks) is typically needed to capture them. This increases the patient's discomfort as well as the cost of monitoring. Even so, seizures might not occur in some cases. Thus, the possibility to estimate the EZ from non-invasive interictal electrophysiological data would be crucial for patients with inconclusive MRI, as this would limit the use of invasive procedures and reduce the need for LTM to wait for unpredictable seizures.

Within this scenario, noninvasive diagnostic tools, such as magnetoencephalography (MEG) as well as low-density (LD-EEG) and high-density electroencephalography (HD-EEG), are becoming of high importance in the presurgical evaluation of patients with drug resistant epilepsy (DRE) undergoing surgery. Electric and Magnetic Source Imaging (ESI/MSI) of interictal epileptic activity have shown promising findings in the delineation of the epileptogenic focus (Abdallah et al., 2017, Bast et al., 2004, Megevand and Seeck, 2018, Murakami et al., 2016, Pellegrino et al., 2018, Tamilia et al., 2018, Tamilia et al., 2020). In patients with normal or non-focal MRIs, several studies highlighted the role of MSI (Bagić, 2016, Funke et al., 2011, Jung et al., 2013, Minassian et al., 1999, Mohamed et al., 2020, RamachandranNair et al., 2007, Seo et al., 2011, Widjaja et al., 2013, Wilenius et al., 2013). Yet, only one assessed the clinical utility of ESI but without any comparative results between LD-EEG and HD-EEG (Brodbeck et al., 2010), while another evaluated both ESI and MSI in simultaneous HD-EEG and MEG recordings (Plummer et al., 2019). None of the aforementioned studies quantified and compared the localization accuracy of non-invasive source imaging against the ground truth given by the patient's icEEG LTM and surgical resection using quantitative

metrics (i.e. distances). Moreover, ESI and MSI findings, such as for example equivalent current dipoles (ECDs), can depict a combination of the EZ and some of its propagation zone (Abdallah et al., 2017). Thus, new metrics, such as dipole clustering, are needed that can offer a quantitative index of the epileptogenicity of the area where the dipole is pointing out. This is particularly important in patients in whom MRI did not show a lesion that could guide the placement of icEEG or surgery.

The aim of this study is to assess the clinical utility of interictal ESI and MSI using dipole clusterness in children and young adults with DRE having inconclusive MRI findings. Our hypothesis is that clustered dipoles with ESI and MSI can accurately estimate the EZ and help optimizing the surgical outcome in these challenging pediatric cases. To test our hypothesis, we retrospectively analyzed interictal LD-EEG, HD-EEG, and MEG data from children and young adults with DRE and inconclusive MRI, along with their icEEG findings from their LTM, their surgical resection, and post-surgical seizure outcome. We localized interictal epileptiform discharges (IEDs) from scalp LD-EEG (19 channels), HD-EEG (72 channels), and MEG (306 sensors) with ESI and MSI respectively using ECDs. For each modality, we computed the dipole clustering, and divided dipoles into clustered and scattered. Then, we compared the localization of clustered and scattered dipoles with the ground-truth SOZ and irritative zone (IZ) defined by long-term icEEG. Finally, we quantified the distances between the surgical resection and ESI (for both LD-EEG and HD-EEG) as well as MSI solutions and assessed their correlation with outcome.

2. Material and methods

2.1. Patient cohort

We retrospectively reviewed the data of pediatric patients with DRE that underwent epilepsy surgery in Boston Children's Hospital (BCH) from July 2012 to June 2018. Patients were included if meeting the following inclusion criteria: (i) had MRI that was negative, showed a subtle lesion of doubtful clinical significance, or provided non-focal inconclusive findings; (ii) underwent presurgical simultaneous HD-EEG and MEG recordings; (iii) underwent epilepsy neurosurgery for resection of the epileptogenic foci; and (iv) had a post-surgical follow up of at least two years. The exclusion criteria were the presence of extensive artifacts and absence of IEDs in the MEG or HD-EEG recordings. The study protocol received approval by the BCH Institutional Review Board (IRB-P00022114: PI: C. Papadelis), which waived the need for written informed consent due to the study's retrospective nature.

2.2. MRI evaluation

MRI studies were performed before and after surgery following an epilepsy specific protocol on a 3 Tesla scanner used in our institution (Prabhu and Mahomed, 2015). The MRI report most proximate to the surgery was pulled from our hospital's database. The information was crosschecked with the summary presentation of the patient's findings at presurgical evaluation conducted by the multidisciplinary epilepsy surgery team. During the above mentioned presurgical evaluation process, MRIs were reviewed with particular focus on possible epileptogenic lesions. We will refer to this reading, guided by detailed clinical information and other neurophysiological techniques (e.g. LTM video or EEG), as the second reading. Finally, the MRIs were retrospectively reviewed by a

subspecialized neuroradiologist (S.P.) at the time of this study. We will refer to this last review as the third MRI reading. The patient's MRIs were characterized as normal, with subtle lesions, or non-focal. Normal MRIs were those that were characterized as such by all reviewers (prospectively and retrospectively). Subtle lesion MRIs were those for which a subtle lesion with unknown clinical significance was mentioned on the report. If the report was negative and the second or third review by the epilepsy specialized neuroradiologist indicated a subtle suspicious area, the MRI was also characterized as having a subtle lesion. Non-focal MRIs were those for which the abnormalities were diffuse and were not indicative of any focal cause of epilepsy, such as diffuse white matter traumatic lesions. MRIs with large lesions (as hemimegalencephaly or multifocal epileptogenic lesions as in tuberous sclerosis) were not considered as non-focal and such patients were not included in this study.

2.3. Simultaneous HD-EEG and MEG recordings

The simultaneous MEG/HD-EEG recordings were conducted at the MEG Core Laboratory of Athinoula Martinos Center for Biomedical Imaging (Charlestown, MA). The guidelines of the International Federation of Clinical Neurophysiology (Hari et al., 2018) were followed for the HD-EEG and MEG recordings. MEG recordings were performed inside a three-layer magnetically shielded room (Imedco, Hägendorf, Switzerland) with a whole-head 306-sensor system (VectorView, Elekta Neuromag, Helsinki, Finland). The system is equipped with 204 planar gradiometers and 102 magnetometers over 102 locations. A non-magnetic 70-channel electrode cap (EASYCAP, Herrsching, Germany) was used to simultaneously record HD-EEG with two additional electrodes (T1 and T2) placed at temporal regions. Nose reference was used for the EEG recordings. Four head position indicator (HPI) coils were placed on the head. The relative locations of the HPI coils and EEG electrodes with respect to anatomical landmarks on patient's head were determined using a three-dimensional (3D) digitizer (FASTRAK®, Polhemus, VT). This allowed aligning the MEG, EEG, and MRI coordinate systems. Horizontal and vertical eye movements were measured via electrooculography. Cardiac activity was measured via electrocardiogram. The patients, having come to the hospital with partial sleep deprivation, were lying in a supine position and were instructed to rest or sleep during the recording. More details about the followed protocol can be found elsewhere (Papadelis et al., 2016). Signals were gathered in 10–12 recordings for each patient lasting 4–5 min each. The head position was reassessed before starting each session. The sampling rate was 1000 Hz. An online low-pass Infinite Impulse Response (IIR) filter of 6th order at 400 Hz was applied during recording.

2.4. Identification of IEDs

A minimum of 30 minutes from the HD-EEG/MEG recordings were extracted by the attending epileptologist as described previously (Tamilia et al., 2020). Data portions with technical disruptions and major artifacts were excluded from further analysis. Two experts (G.N., C.P.) retrospectively reviewed these segments and marked the IEDs. Both readers were blind to the resection and patient's outcome, as well as to each other's markings. For data visualization and reading, we applied the following filters in *Brainstorm*: DC offset; band-pass filter: 1–70 Hz; and notch filter: 60 Hz and harmonics (Tadel et al., 2011). Each modality was read independently and the marking of the IEDs was performed following established criteria (Chatrian, 1974): (i) paroxysmal occurrence; (ii) abrupt change in polarity; (iii) duration <200 ms; and (iv) scalp topography consistent with a physiologic field. For the HD-EEG review, we used both an average montage and bipolar montages.

For the MEG review, the 306 sensors were divided into eight regions that consist of 38–39 channels each (right- and left-temporal, right - and left-frontal, right - and left-parietal, right - and left-occipital). For both modalities, the reviewers read the recordings region by region and marked the peak of the main spike deflection, aiming for the best combination of the most prominent and the earliest activity, depending on the reviewer's judgment. For MEG, the signal space projection technique was used to reject external disturbances (Uusitalo and Ilmoniemi, 1997) due to cardiac events detected by the electrocardiography. For EEG, any portion of data contaminated by biological artifacts (e.g. heartbeat or eye movements) was excluded. IED marking and following source imaging were performed retrospectively.

2.5. Source localization of IEDs

2.5.1. Forward model

Brainstorm software was used to co-register the patient's head points, digitized at the time of the recording, with the MRI (Tadel et al., 2011). We used the pre-operative patient's MRI to construct a realistic head model using *OpenMEEG* (Gramfort et al., 2010). *Freesurfer* and its automatic segmentation pipeline software was used to extract the individual cortical surfaces from the MRI volume with default parameter settings (Dale et al., 1999). Deeper and subcortical brain regions were considered by generating a grid of points in reference to the full brain volume (volume points) through an adaptive integration method implemented in *Brainstorm*. A three-layer boundary elementary model (BEM) was used for the ESI and MSI.

2.5.1.1. Equivalent current dipoles. We localized the source of each IED using a dipole scanning method that is available in *Brainstorm* (Tadel et al., 2011). This method selects the most significant dipole in a 3D grid of dipoles that are already estimated. The grid was reconstructed from the entire brain volume of each patient's MRI with a spatial resolution of 5 mm. We decided to localize each individual IED and not the average to avoid merging IEDs originated from different sources (Diekmann et al., 1998, Tamilia et al., 2019). To assess the utility of HD-EEG in comparison to LD-EEG, we performed the ESI analysis using both all available EEG channels (72 channels) as well as 19 channels selected according to the 10–20 system. Unconstrained source analysis was performed using dipole scanning across 25 ms backwards from marked peak of the IED and selecting the time point providing the ECD with the highest Goodness of Fit (GOF). Finally, only dipoles with a GOF $\geq$ 60% were kept for further analysis (Alhilani et al., 2020, Tamilia et al., 2019, Tamilia et al., 2020). The IEDs identified with the EEG and those identified with the MEG were localized independently.

2.5.2. Dipole clustering

For each dipole, separately for ESI (both for LD-EEG and HD-EEG) and MSI, we calculated the number of dipoles, which are clustered around it, i.e. the number of dipoles that were located within a distance of 15 mm from it (Fig. 1a). Then, we normalized this measure by dividing it with the patient's total number of dipoles (range: 0–1). We will refer to such a normalized measure as the "clusterness" of the dipole (the higher the number, the more the dipole was surrounded by other dipoles). The cut-off of 15 mm is based on previous studies, which report such a distance as the width of a gyrus (based on the mean width of the parahippocampal gyrus) (Ono et al., 1990), and thus implies that the dipoles are close to each other within a gyral width even if not necessarily located in the same gyrus (Kim et al., 2016, Tamilia et al., 2019).
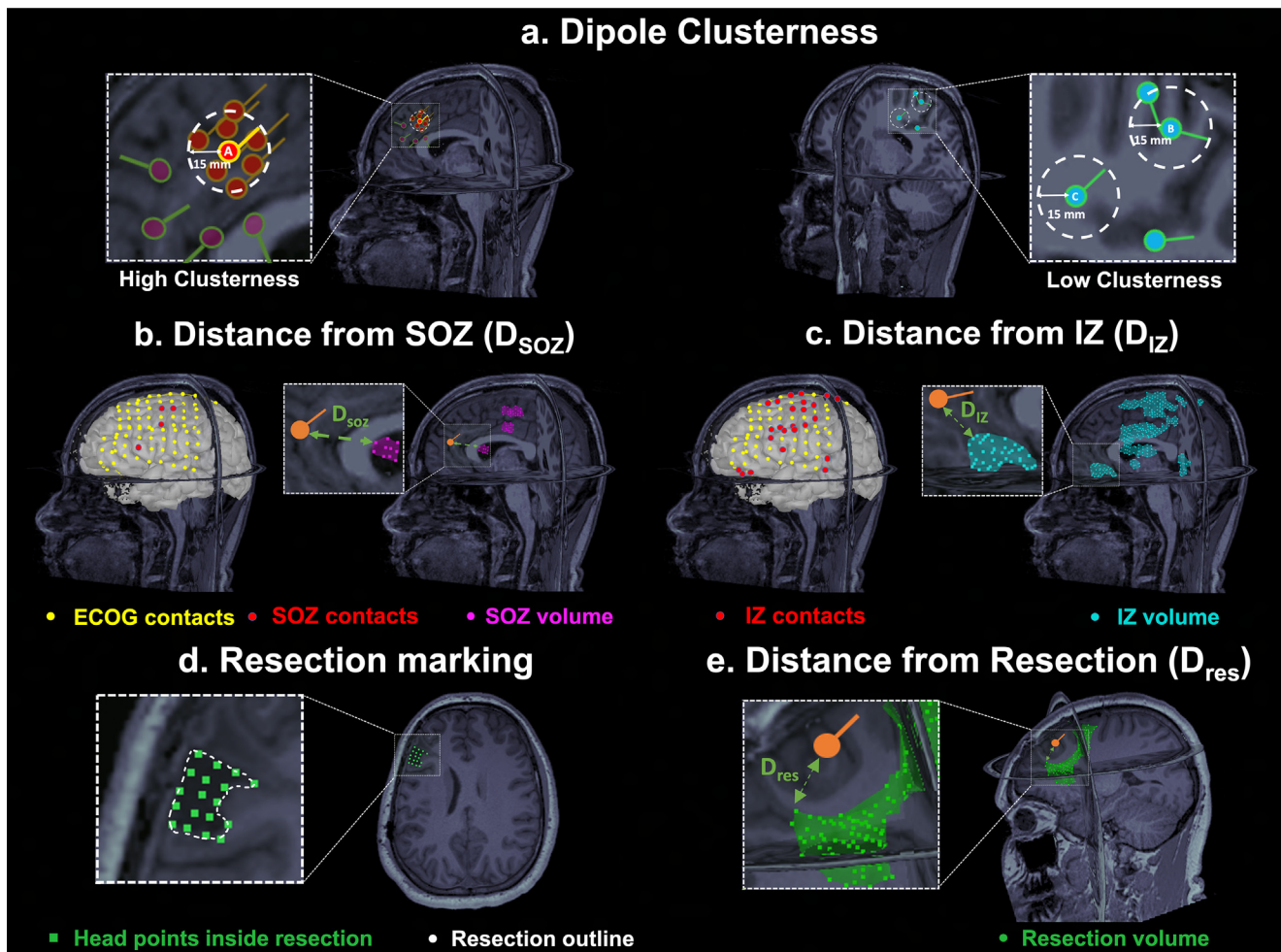
Fig. 1. Estimation of Dipole Clusterness and Distances from Seizure Onset Zone (D$_{SOZ}$), Irritative Zone (D$_{IZ}$), and Resection (D$_{res}$). (a) Left: Example of a dipole (dipole A) with high clusterness, i.e. high number of surrounding dipoles (n = 7) within a radius of 15 mm (white dash circle). Dipoles which are outside the 15-mm radius of dipole A do not contribute to clusterness. Right: Example of dipoles with low clusterness (i.e. with one or two surrounding dipoles). (b) Intracranial EEG (icEEG) contacts belonging to the Seizure Onset Zone (SOZ) (in red) defined the SOZ volume (purple) in Magnetic Resonace Imaging (MRI) space. Euclidian distance (green arrow) of each dipole (orange) from the closest point of the SOZ volume was computed (D$_{SOZ}$). (c) icEEG contacts belonging to the Irritative Zone (IZ) (in red) defined the IZ volume (cyan). Euclidian distance (green arrow) of each dipole from the closest point of the IZ volume was computed (D$_{IZ}$). (d) Definition of the resected cavity (green points) on the postoperative MRI after its coregistration with the preoperative MRI. (e) Euclidian distance (green arrow) of a dipole (orange) from the closest point of the resection (D$_{RES}$).

2.6. Validation of ESI and MSI against the SOZ and IZ defined by long-term icEEG

To validate the ESI and MSI solutions in terms of their accuracy to localize the SOZ and IZ, we used as ground-truth the SOZ and IZ that had been prospectively determined during each patient's long-term icEEG monitoring, independently from this study.

2.6.1. Localization of icEEG contacts

Per BCH clinical practice, icEEG LTM is performed with subdural grids and strips and/or depth electrodes for stereo EEG, after consensus of the multidisciplinary epilepsy surgery conference, when there is perceived need for a better definition of the epileptogenic focus and/or the functional anatomical regions (Alhilani et al., 2020, Tamilia et al., 2019, Tamilia et al., 2018). Therefore, the placement of icEEG electrodes was performed independently from this study and was planned prospectively during the epilepsy conference by a team of experts consisting of pediatric epileptologists, neurosurgeons, neuropsychologists, neuroradiologist, and other practitioners. For this study's purposes, we fused the post-implantation Computational Tomography (CT) scan (voxel size = 0.5 × 0.5 × 0.5 mm) with the presurgical MRI using *Brainstorm* (Tadel et al., 2011) in order to document the electrodes locations.

We identified the coordinates of each contact through visual review of the fused CT-MRI image on axial, coronal, and sagittal planes. We reconstructed the patient's cortical surface from his/ her preoperative MRI using *Freesurfer* and mapped each contact location on the 3D brain model (Dale et al., 1999).

2.6.2. Definition of the SOZ and IZ

Per BCH clinical practice, pediatric epileptologists reviewed all the ictal EEG segments of the patient throughout the LTM period and identified the SOZ as the icEEG contact(s) showing the earliest change in activity associated with clinical or subclinical seizures (Alhilani et al., 2020). Similarly, the IZ was defined as the icEEG contacts recording spikes after review of interictal activity over different days (Alhilani et al., 2020). The delineation of these zones was performed pre-surgically and was taken into consideration during the surgical planning. For the purposes of this study, SOZ and the IZ were then delineated in the 3D MRI space for each patient by including a volume up to 5 mm surrounding the center of each SOZ and IZ contact.

2.6.3. ESI/MSI distance

For each dipole/IED source, we calculated the distance from the SOZ (D$_{SOZ}$) as the Euclidean distance from the closest point of the

SOZ volume (Fig. 1b). Sources with $D_{SOZ} \leq 15$ mm were classified as concordant to the SOZ, or outside the SOZ otherwise. The percentage of concordant dipoles was used to evaluate the precision of each modality (ESI and MSI). Similarly, the distance from the IZ (D_{IZ}) was calculated for each dipole (Fig. 1c), and the precision to the IZ was estimated for ESI and MSI. ESI and MSI dipoles were analyzed separately.

2.6.4. Receiver Operating Characteristic (ROC) curve analysis

A receiver operating characteristic (ROC) curve analysis was performed to evaluate how accurately the measure of *clusterness* localizes the SOZ (i.e. distinguishes dipoles inside and outside the SOZ). ROC analysis was performed separately for LD-EEG, HD-EEG and MEG, according to the notion that the dipole clusterness should be larger in the EZ compared to the other sites. Therefore, we regarded as: (i) true positive, the dipoles that were concordant with the SOZ and had high clusterness; (ii) false positive, the dipoles that were not concordant with the SOZ but had high clusterness; (iii) true negative, the dipoles that were outside the SOZ and had low clusterness; and (iv) false negative, the dipoles that were inside the SOZ and had low clusterness. The performance of *clusterness* to localize the SOZ was quantified by the area under the curve (AUC) of the ROC curve. With a given cut-off threshold, which we defined by the Youden's J statistic, we divided the dipoles in *clustered* (high clusterness) and *scattered* (low clusterness) (Fig. 1a), and estimated the sensitivity and specificity of the clustered dipoles for the SOZ localization. The same ROC analysis was also performed for the IZ.

2.7. Correlation of ESI and MSI with resection and outcome

We defined the resection volume by co-registering the presurgical and postsurgical MRI and by marking all the volume points corresponding to the resection cavity (Fig. 1d) blindly to the ESI and MSI results and to the outcome. For each dipole, we calculated the distance from resection (D_{RES}) as the Euclidean distance between each dipole's coordinates and the closest point of the resection volume (Fig. 1e). Dipoles with $D_{RES} < 15$ mm were classified as resected or non-resected (Alhilani et al., 2020, Tamilia et al., 2019). The resection percentage of ESI and MSI was calculated as the percentage of resected dipoles on the total number of dipoles. The resection percentage was also calculated separately for clustered or scattered dipoles, which were distinguished based on the SOZ ROC curve analysis described above.

A board-certified pediatric epileptologist (J.B.) used the standardized Engel scale to evaluate each patient's post-surgical outcome from their most recent follow-up visit. Patients were distinguished in *optimal* and *suboptimal* outcome, with the Engel scores being 1 for the optimal outcome group and Engel 2 or 3 for the suboptimal outcome group (Engel et al. 1993). No patients with Engel 4 score were seen in our cohort.

2.8. Statistical analysis

We used Kruskal-Wallis test with post-hoc Tukey-Kramer analysis to compare continuous variables between modalities (LD-EEG vs. HD-EEG vs. MEG). We used Wilcoxon rank sum test to compare continuous or discrete variables between groups of patients (optimal vs. suboptimal outcome). Normality of the distribution was assessed by Shapiro-Wilk test, and non-parametric statistics was used since the variables did not follow standard normal distribution. To test whether D_{RES} can predict the patient's outcome, we used a logistic regression model of the probability of optimal outcome as function of the D_{RES} separately for the LD-EEG (ESI), HD-EEG (ESI) and MEG (MSI). Binary logistic regression was also used to assess the predictive effect of the brain's resected volume on

patients' outcome. Binary logistic regression was also performed to verify the presence of any relationship between the clusterness of each dipole and their proximity to the SOZ or IZ (D_{SOZ} or D_{IZ}). The chi-square test with Bonferroni correction for multiple comparisons was used to compare percentages between modalities (LD-EEG vs. HD-EEG vs. MEG) or between outcomes groups (optimal vs. suboptimal outcome). Bonferroni correction was applied in case of multiple comparisons. A *p*-value < 0.05 was considered statistically significant. Results are expressed as median (inter-quartile range, IQR) or mean ± standard deviation (SD). SPSS statistics (version 23, IBM, New York, USA) was used for statistical analysis.

3. Results

3.1. Patient cohort

During the selected period, 30 patients with normal or non-focal MRI underwent presurgical evaluation. Of these patients, 19 did not meet our inclusion criteria due to: (i) a lesion found on MRI during the second or third reading (n = 4); (ii) not having MEG during the presurgical evaluation (n = 7); (iii) not having HD-EEG during the presurgical evaluation (n = 2); and (vi) not having undergone brain surgery after the evaluation (n = 6). As a result, 11 children and young adults (4 females) were included in our study. Table 1 describes the patient cohort demographics and clinical information. For patients 1 and 7, no seizures were captured during the LTM or only short intra-operative monitoring had been performed, thus they were excluded from the comparison with the icEEG-defined ground-truth (SOZ and IZ). Mean age of diagnosis was 7.1 (range: 1–16) years, mean duration of epilepsy before surgery was 6.4 (range: 2–12) years and mean age at surgery was 13.5 (range: 4–21) years. MRIs were characterized as normal in four patients. Subtle lesions were found in six patients and one patient had non-focal (diffuse) white mater lesions after head trauma. Five children had the SOZ overlapping with the eloquent cortex, which lead to incomplete SOZ resection. Histology of the resected brain was available for eight children and showed cortical dysplasia pathology in three (37.5%), gliosis in four and reactive changes due to history of head trauma in one patient. Three patients had laser ablation and no brain tissue was sent for histology. The mean follow-up was 3.5 (range: 1–7) years. The surgical outcome was Engel 1 (free of disabling seizures) in 36% (4 out of 11) of the patients, Engel 2 (rare disabling seizures) (3 out of 11) in 27% of the patients (one patient was 2a while the other two were 2b), and Engel 3 (worthwhile improvement) in 36% (4 out of 11) of the patients. The seizure status of all patients was improved after surgery (none of the patients was Engel 4). No correlation was found between the resection volume and the surgical outcome (OR: 1.068, p = 0.455).

3.2. IEDs on EEG and MEG

We marked 1249 IEDs for the EEG (mean: 113.5) and 1726 IEDs (mean: 159.9) for the MEG. The rate of IEDs was 3.2 IEDs/min for the EEG and 4.5 IEDs/min for the MEG. We localized all the IEDs using both the LD-EEG as well as the HD-EEG recordings and accepted for further analysis (GOF > 60%) a total of 1243 for the LD-EEG (mean: 113), 1146 dipoles for the HD-EEG (mean: 104.2), and 1357 dipoles for the MEG (mean: 123.4). The localized events were 9 ms before the marked peak of the spike for the LD-EEG (p < 0.001), 7 ms for the HD-EEG (p < 0.001), and 4 ms for the MEG (p < 0.001). Patient #1 had a remarkably high rate of IEDs per minute (for EEG: 30.1 IEDs/min, for MEG: 36.9 IEDs/min); for this patient, 15 min of recordings were included in the analysis.

Table 1
Demographics and Clinical Features of our patients' cohort.

Patient	Sex	Age of epilepsy onset	Age	Outcome (Engel)	Follow-up [years]	SOZ location [a]	IZ location [a]	SOZ Resection	Surgical resection location (lobar-sublobar level)	Resected Volume [%]	MRI findings	Histopathological Diagnosis
1	Male	6	10	1a	5	–	Frontal/Parietal (R)	–	Frontal/ Parietal/ Temporal (R)	1.2%	Normal	Gliosis, inflammatory changes
2	Female	2	18	1a	7	Mesial, anterior and inferior Temporal (L)	Temporal (L)	Complete**	Anterior Mesial Temporal (L)	2.1%	Subtle	Gliosis
3	Male	7	15	2a	5	Mesial Temporal (L), Lateral Frontal (L)	Anterior, inferior, mesial Temporal (L). Subfrontal (L)	Partial*	Anterior Temporal, Hippocampus, Amygdala (L)	1.3%	Normal	FCD 1a
4	Male	7	16	3	3	Lateral Frontal (L)	Lateral Frontal (L)	Partial*	Frontal (L)	0.8%	Subtle	Gliosis
5	Male	12	17	3	3	Insula (L)	Insula (L)	Partial*	Superior/ Posterior Insula (L)	0.5%	Normal	–
6	Female	8	15	1a	3	Lateral Temporal (L), Orbital, middle Frontal (L)	Temporal (L), Frontal (L)	Complete**	Middle Frontal gyrus, anterior-inferior Frontal gyrus, and lateral orbitofrontal cortical regions (L)	1.6%	Subtle	Suboptimal specimen orientation or Subtle cortical malformation
7	Male	4	7	3	3	(no invasive LTM) Temporal (both sides, left predominance)- scalp EEG (phase 1)	(no invasive LTM) mesial Temporal (L) (intraoperative iEEG)	Partial	Anterior, mesial Temporal (L)	1.7%	Subtle	Gliosis
8	Male	9	15	2b	3	Mesial Temporal (L), Parietal (L), Occipital (L).	Mesial Temporal (L), Parietal (L), Occipital (L).	Partial	Occipital, Parietal, Temporal (L)	1.2%	Normal	–
9	Female	8	21	2b	4	Superior lateral Frontal and contiguous interhemispheric areas (R)	Superior lateral Frontal and contiguous interhemispheric areas (R)	Partial*	Anterior Frontal (R)	2.3%	Non-focal (multiple white matter traumatic lesions)	Reactive changes related to the history of the head trauma.
10	Female	3	4	1a	1	Insula (R), inferior frontal gyrus (R), cingulate region (R), Hippocampus (R)	Insula (R), inferior frontal gyrus (R), cingulate region (R), Hippocampus (R)	Complete**	Posterior Insula (R)	0.7%	Subtle	–
11	Male	5	10	3	1	Precentral Sulcus (L), Superior frontal Sulcus (L)	Superior, pre and post central gyrus, angular gyrus (L), interhemispheric regions (L)	Partial*	Frontal (R)	0.9%	Subtle	FCD1

*Due to overlapping with eloquent cortex.
**Some of the electrodes reported as the SOZ in the LTM were prioritized over others during the surgical conference following a multimodal approach.
*** The areas pointed by most active electrodes were resected even though no seizures were captured during the LTM.
- The patient had ablation and no histopathological information were collected.
Patient 7 did not undergo invasive long-term monitoring (LTM) but he had LTM with scalp EEG.
[a] SOZ and IZ were defined based on the invasive LTM report. [b] Surgical resection location defined by the surgical notes found in patient's records. L: left, R: Right, SOZ: Seizure Onset Zone, IZ: Irritative Zone, MRI: Magnetic Resonance Imaging, LTM: Long Term Monitoring.

3.3. Concordance of ESI and MSI with ground truth SOZ

When considering all the dipoles without accounting for their clustering, the D_{SOZ} did not differ between ESI and MSI while HD-EEG outperformed LD-EEG ($p < 0.05$) [LD-EEG ESI: median: 24.3 (26.7) mm; HD-EEG ESI: median: 20.6 (21.8) mm; MSI: median: 21.4 (23.7) mm]. Comparing D_{SOZ} in individual patients, we observed that MEG outperformed HD-EEG ($p < 0.05$) in two cases

(22.2%) with a mean improvement of 15.4 mm, HD-EEG outperformed MEG in four cases (44.4%) ($p < 0.05$) with a mean improvement of 6.5 mm, while no difference was found in three cases (33.3%). Comparing HD-EEG with LD-EEG ESI, we found that HD-EEG was better than LD-EEG ESI in two cases (22.2%) with mean improvement of 4.9 mm ($p < 0.05$) while no significant difference was found in seven cases (77.8%). MEG outperformed LD-EEG ESI in two cases (22.2%) with mean improvement of 54.6 mm

(p < 0.05), LD-EEG ESI was closer to the SOZ in two cases (22.2%) with mean improvement of 11.8 mm (p < 0.05), while no difference was found in five cases (55.6%). In terms of precision to the SOZ, when all dipoles were included in the analysis, no difference was found between ESI (LD-EEG: 29%; HD-EEG: 34%) and MSI (MEG: 29%) (p > 0.05).

Clusterness was negatively correlated with the D_{SOZ} for both ESI (LD-EEG: R = −0.41, p < 0.001; HD-EEG: R = −0.42, p < 0.001) and MSI (R = −0.4, p < 0.001). For both ESI and MSI, the clusterness of dipoles inside the SOZ was higher than outside [LD-EEG ESI: 7.1% (10.1%) vs. 2.2% (6.1%) p < 0.001; HD-EEG ESI: 10.3% (24%) vs. 3.2% (10.9%), p < 0.001; MSI: 11.3% (14.1%) vs. 5% (13.3%), p < 0.001] (Fig. 2a). Post-hoc analysis showed no difference between HD-EEG ESI and MSI (p > 0.05), while both outperformed LD-EEG ESI for dipoles inside the SOZ (p > 0.05). For dipoles outside the SOZ, MSI showed higher clustering than ESI, while HD-EEG outperformed LD-EEG ESI (p < 0.05). ROC analysis showed that dipole clusterness distinguished dipoles inside vs. outside the SOZ with an AUC of 0.7 and 0.69 for LD-EEG and HD-EEG ESI respectively and 0.64 for MSI (Fig. 2b). The best cut-off value of clusterness to localize the SOZ was equal to 3.1% for the LD-EEG ESI, 5.4% for the HD-EEG ESI and 8.6% for the MSI. Clustered dipoles (i.e. dipoles with clusterness ≥ cut-off) provided a sensitivity and specificity to the SOZ of 69.1% and 61.5% for the LD-EEG ESI, 65% and 60.7% for the HD-EEG ESI, and 74.4% and 49% for the MSI respectively. When evaluating the degree of clusterness for each modality, MSI had no difference in the percentage of clustered dipoles compared to HD-EEG ESI [MEG: 62.9% (854/1357); HD-EEG: 59.9% (686/1145), p > 0.05] while LD-EEG ESI had lower percentage of clustered dipoles compared to both modalities [MEG: 62.9% (854/1357) vs. LD-EEG: 50.1% (623/1243), p < 0.001; HD-EEG: 59.9% (686/1145)

vs. LD-EEG: 50.1% (623/1243), p < 0.001]. Clustered dipoles showed a higher precision to the SOZ than scattered dipoles for both the LD-EEG ESI (43.5% vs. 14.8%, p < 0.001), HD-EEG ESI (49.7% vs. 21%, p < 0.001), and for MSI (43% vs. 22.3%, p < 0.001) (Fig. 2c). No differences in precision to the SOZ was found between modalities for the clustered dipoles (p > 0.05). MSI had higher precision to the SOZ of the scattered dipoles compared to LD-EEG ESI (p < 0.05), while no difference was found between the rest of modalities. Clustered dipoles were closer to the SOZ than scattered dipoles for both the ESI [D_{SOZ}: LD-EEG: 16.9 (19) mm vs. 32.5 (30.9) p < 0.001; HD-EEG: 15.5 (12.7) mm vs. 31.4 (27.7) mm, p < 0.001] and MSI [D_{SOZ} = 16.2 (12) mm vs. 30.4 (30.9) mm, p < 0.001] (Fig. 2d). For the clustered dipoles, HD-EEG outperformed LD-EEG ESI (p < 0.05), while no difference was found between the rest modalities (p > 0.05). For scattered dipoles, HD-EEG ESI and MEG outperformed LD-EEG ESI (p < 0.05) while no difference was found between HD-EEG ESI and MSI.

3.4. Concordance of ESI and MSI with ground truth IZ

For the IZ localization, when considering all dipoles without accounting for their clustering, MSI and HD-EEG ESI outperformed LD-EEG ESI (p < 0.05), while no difference was found between MSI and HD-EEG ESI (p > 0.05) [LD-EEG ESI: 18.4 (22.6) mm, HD-EEG ESI: 16.7 (18) mm; MSI: 15.6 (16.4) mm].

Comparing D_{IZ} in individual patients, we observed that MSI outperformed HD-EEG ESI (p < 0.05) in three cases (30%) with a mean improvement of 35.5 mm, HD-EEG ESI outperformed MSI in three cases (40%) (p < 0.05) with a mean improvement of 19.6 mm, and no difference was found between MSI and HD-EEG ESI in three cases (30%). Comparing LD-EEG with HD-EEG ESI, we found that
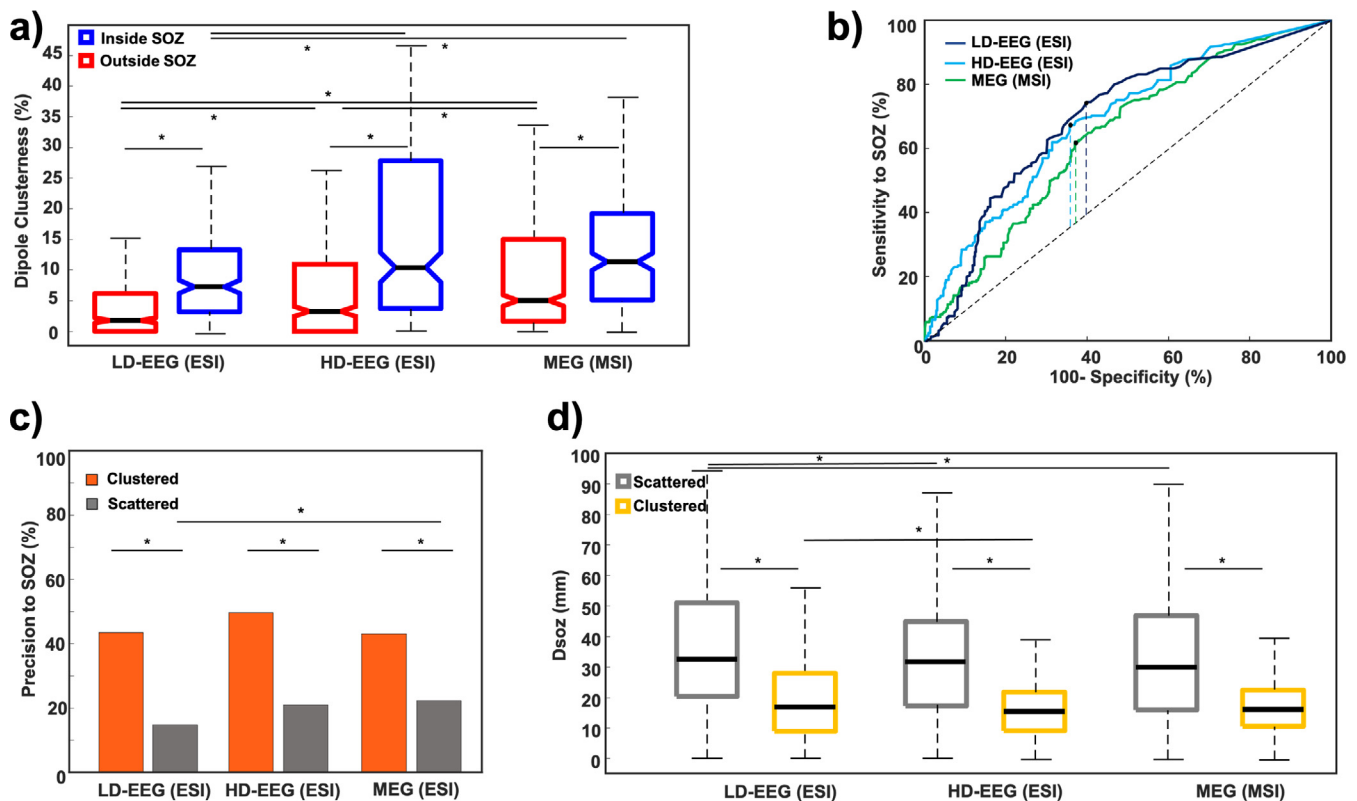

Fig. 2. Validation of Electric Source Imaging (ESI) with Low-Density EEG (LD-EEG) and High-Density EEG (HD-EEG) as well as Magnetic Source Imaging (MSI) with magnetoencephalography (MEG) against the ground truth given by the Seizure Onset Zone (SOZ). (a) Comparison of dipole clusterness inside (blue) and outside (red) the SOZ for ESI and MSI. (b) Receiver operating characteristic (ROC) curves built on ESI with LD-EEG (dark blue), HD-EEG (cyan) and MSI with MEG (green) dipole clusterness to identify the SOZ. Dashed vertical lines mark the Youden's Index. (c) Precision to the SOZ for clustered (orange) and scattered (grey) dipoles for ESI and MSI. (d) Distance from the SOZ for clustered (yellow) and scattered (grey) dipoles. Stars indicate significant differences (p-values < 0.05).

HD-EEG was better than LD-EEG ESI in three cases (30%) with mean improvement of 12.9 mm (p < 0.05), while no difference was found in seven cases (70%). MEG outperformed LD-EEG ESI in two cases (20%) with mean improvement of 43.8 mm (p < 0.05), LD-EEG ESI was closer to SOZ in one case (10%) with mean improvement of 7.5 mm (p < 0.05), while no difference was found in seven cases (70%). In terms of precision to the IZ, HD-EEG outperformed LD-EEG ESI (49% vs. 41%, p < 0.05), while no difference was found between the rest of modalities (p > 0.05).

Dipole clusterness was negatively correlated with the D_{IZ} for both ESI (LD-EEG: −0.42, p < 0.001; HD-EEG: R = −0.403, p < 0.001) and MSI (R = −0.44, p < 0.001). For both ESI and MSI, the clusterness of dipoles inside the IZ was higher than outside [LD-EEG ESI: 7.2% (11.2%) vs. 1.6% (4.1%) p < 0.001; HD-EEG ESI: 10.5% (22.8%) vs. 2.6% (5.6%); MSI: 11.9% (14.6%) vs. 4.3% (9%), p < 0.001] (Fig. 3a). No difference was found between HD-EEG ESI and MSI (p > 0.05) while both outperformed LD-EEG ESI for the dipoles inside the IZ (p > 0.05). For dipoles outside the IZ, MSI showed higher clustering than ESI, while HD-EEG outperformed LD-EEG ESI (p < 0.05).

ROC curve analysis showed that dipole clusterness distinguished dipoles inside and outside the SOZ with an AUC of 0.74 for LD-EEG ESI and 0.75 with the HD-EEG ESI and 0.72 for MSI (Fig. 3b). The best cut-off value of clusterness to localize the IZ was equal to 3.9% with LD-EEG ESI, 5.2% for HD-EEG ESI, and 7.3% for MSI. MSI had no difference in the clustered dipoles percentage compared to HD-EEG ESI [MEG; 65.5% (889/1357); HD-EEG; 62.5% (716/1145), p > 0.05], while LD-EEG ESI had lower clustered dipoles percentage compared with both modalities [MEG: 65.5% (889/1357) vs. LD-EEG: 45.2% (562/1243), p < 0.001; HD-EEG: 62.5% (716/1145) vs. LD-EEG: 45.2% (562/1243), p < 0.001]. Clustered dipoles (i.e. dipoles with clusterness ≥ cut-off) provided a sensitivity and specificity to the IZ of 67.7% and 73.1% for the LD-EEG ESI, 71.4% and 72.1% for the HD-EEG ESI, and 67.5% and 69.5% for the MSI respectively.

Clustered dipoles showed a higher precision to the IZ than scattered dipoles for both the LD-EEG ESI (64% vs. 23.8%, p < 0.001) and HD-EEG ESI (71.2% vs. 27.7%; p < 0.001) and for MSI (66.4% vs. 29.5%, p < 0.001) (Fig. 3c). No differences were found between modalities for clustered and scattered dipoles (p > 0.005).

Clustered dipoles were closer to the IZ than scattered dipoles for both the ESI [D_{IZ}: LD-EEG: 12.6 (11.4) mm vs. 28 (26.4) mm, p < 0.001; HD-EEG: 11.6 (9.3) mm vs. 24.4 (24.2) mm, p < 0.001] and MSI [D_{SOZ} = 11.6 (8.9) mm vs. 22.8 (24.1) mm, p < 0.001] (Fig. 3d). D_{IZ} for clustered dipoles did not differ between modalities (p > 0.05). For scattered dipoles, D_{IZ} was shorter for MSI than LD-EEG ESI (p = 0.024) while no differences were found between the rest of modalities.

3.5. Correlation of distance from resection (D_{RES}) with outcome

When considering all dipoles (regardless their clusterness), we found that D_{RES} was shorter in optimal compared to suboptimal outcome patients for both ESI (LD-EEG: 18.7 vs. 27.6 mm, p < 0.001; HD-EEG: 9.5 vs. 23.6 mm, p < 0.001) and MSI (10.9 vs. 23.9 mm, p < 0.001) (Fig. 4a). The percentage of dipoles resection was higher in optimal than suboptimal outcome patients (LD-EEG ESI: 42% vs. 25%, p < 0.001; HD-EEG ESI: 67% vs. 31%, p < 0.001; MSI: 66% vs. 32%, p < 0.001). Furthermore, in patients with optimal outcome (who are proof of EZ resection), post-hoc
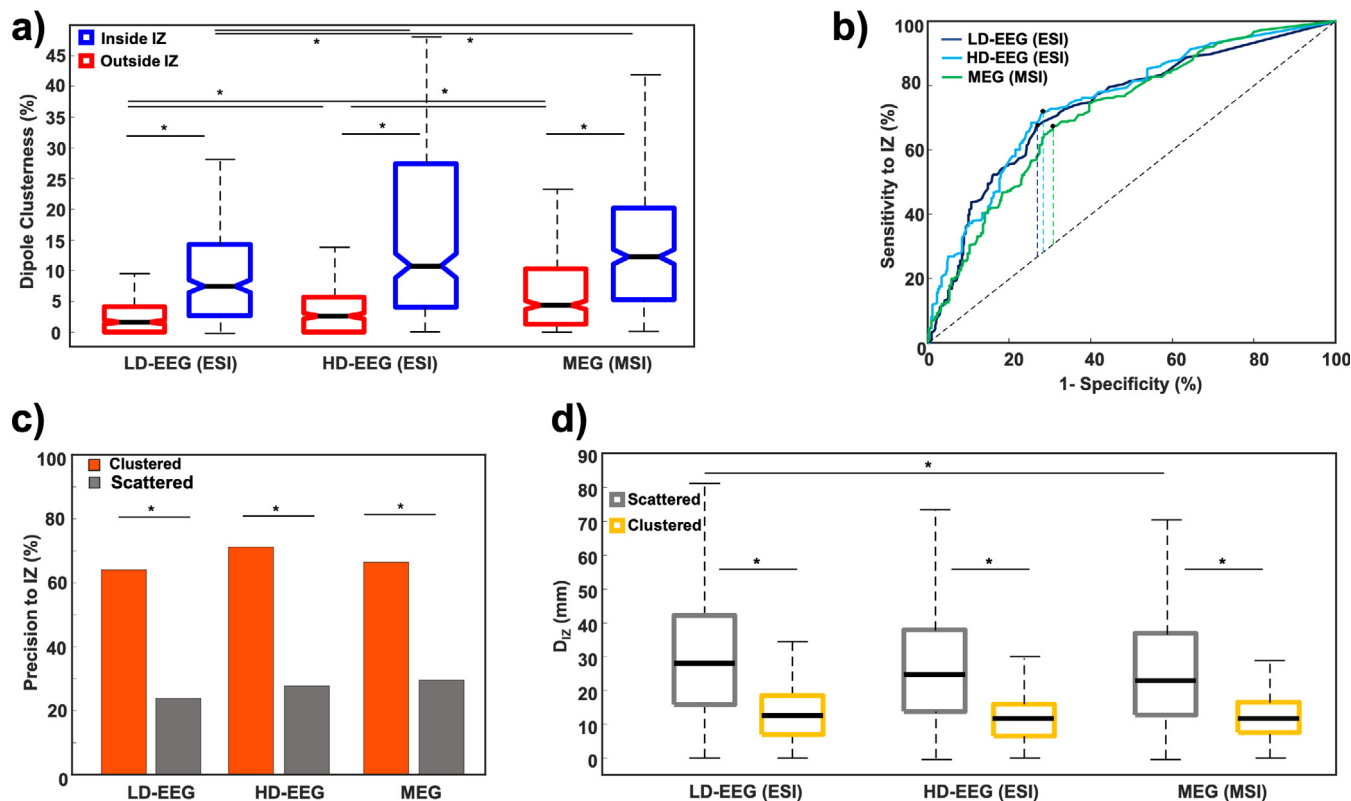

Fig. 3. Validation of Electric Source Imaging (ESI) and Magnetic Source Imaging (MSI) against the ground truth given by the Irritative Zone (IZ). (a) Comparison of dipole clusterness inside (blue) and outside (red) the IZ for ESI and MSI. (b) Receiver operating characteristic (ROC) curves built on ESI with Low-Density EEG (LD-EEG) (dark blue), high-density EEG (HD-EEG) (cyan) as well as magnetic source imaging (MSI) with magnetoencephalography (MEG) (green) dipole clusterness to identify the IZ. Dashed vertical lines mark the Youden's Index. (c) Precision to the IZ for clustered (orange) and scattered (grey) dipoles for ESI and MSI. (d) Distance from the IZ for clustered (yellow) and scattered (grey) dipoles. Stars indicate significant differences (p-values < 0.05).
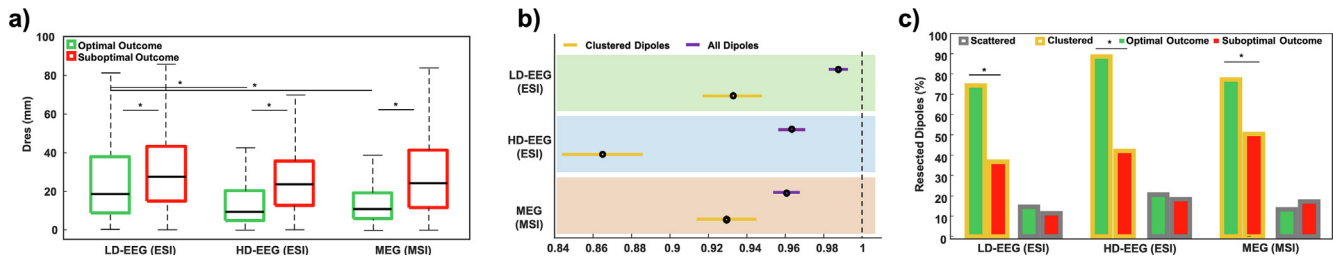
Fig. 4. **Correlation of distance form resection (Dres) with surgical outcome and evaluation of clustering analysis effect.** (a) Patients with optimal (green) and suboptimal (red) surgical outcome for electric source imaging (ESI) with Low-Density EEG (LD-EEG), High-Density EEG (HD-EEG) as well as magnetic source imaging (MSI) with magnetoencephalography (MEG). (b) Logistic regression used to model the probability of good outcome based on D$_{RES}$ of all dipoles (purple) and clustered dipoles (yellow) separately for ESI with LD-EEG (green) and HD-EEG (cyan) and MSI (orange). (b) Prercentage of resected clustered (yellow) and scattered (grey) dipoles in patients with optimal (green) and suboptimal (red) outcome for each modality.

analysis showed that HD-EEG ESI and MSI outperformed LD-EEG ESI (p < 0.001), while no difference was found between HD-EEG ESI and MSI [D$_{RES}$: LD-EEG 18.7 (29.1) mm; HD-EEG 9.5 (15.6) mm; MEG: 10.9 (13.1) mm].

Logistic regression, when all dipoles are included in analysis, showed that D$_{RES}$ predicts outcome for both ESI (LD-EEG: OR = 0.987, CI = 0.982–0.992, p < 0.001; HD-EEG: OR = 0.963, CI = 0.956–0.970, p < 0.001) and MSI (OR = 0.960, CI = 0.953–0.967, p < 0.001) (Fig. 4b). When comparing clustered vs. scattered dipoles, we found that clustered dipoles outperformed scattered ones in patients with optimal outcome as they were closer to resection for both ESI [D$_{RES}$: LD-EEG: 9.3 (10.9) vs. 35.6 (27.4) mm, p < 0.001; HD-EEG: 6.6 (7.2) vs. 30.2 (27.8) mm] and MSI [D$_{RES}$: 9.8 (8.6) vs. 35.1 (31.5) mm, p < 0.001].

For clustered dipoles, the percentage of resection was higher in optimal than suboptimal outcome patients (ESI: LD-EEG: 74.4% vs. 36.8%, p < 0.001; HD-EEG: 88.6% vs. 42.2%, p < 0.001; MSI: 77.3% vs. 50.5%, p < 0.001), while this was not seen for the scattered dipoles (ESI: LD-EEG: 14.7% vs. 11.5%, p > 0.05; HD-EEG: 20.7% vs 18.5%, p > 0.05; MSI: 13.4% vs 17.3%, p > 0.05) (Fig. 4c). Logistic regression showed that D$_{RES}$ of clustered dipoles predicts outcome for both ESI (LD-EEG: OR = 0.932, CI = 0.917–0.948, p < 0.001; HD-EEG OR = 0.861, CI = 0.844–0.886, p < 0.001) and MSI (OR = 0.93, CI = 0.914–0.945, p < 0.001) (Fig. 4b).

4. Discussion

This study demonstrates the clinical value of interictal ESI and MSI in the presurgical assessment of MRI-negative children and young adults with DRE. We assess the localization accuracy of ESI and MSI compared to the gold standard given by the icEEG and surgical resection. Our data indicate that dipole clusterness augments the localization accuracy of both modalities in their contribution to pre-surgical planning. In particular, our ESI and MSI findings show that: (i) the level of clustering of each dipole correlates with its proximity to the intracranially-defined SOZ and IZ, where the highly clustered dipoles can better estimate the SOZ and IZ than the scattered (i.e. scarcely clustered) dipoles; (ii) all three modalities (i.e. LD-EEG, HD-EEG, and MEG) benefit from clusterness measures; (iii) modalities using lower number of sensors (i.e. LD-EEG and HD-EEG) benefit more from clusterness compared to those with higher number of sensors (i.e. MEG); (iv) clustered dipoles are closer to the resection than the scattered dipoles in patients with favorable surgical outcome; (v) the proximity of clustered dipoles to resection is linked to the patient's outcome; and (vi) ESI with HD-EEG and MSI did not reveal significant differences in localizing the SOZ and IZ. These findings indicate that assessing the level of ESI and MSI dipole clusterness allows recognizing the interictal activity generated in the most epileptogenic areas whose removal is associated with favorable outcome.

4.1. Dipole clustering improves the SOZ and IZ localization

Our data show that quantifying the level of clustering of each dipole augments the ability of LD-EEG, HD-EEG, and MEG to localize the EZ. We observed that interictal ESI and MSI localize the SOZ, as defined invasively by the icEEG, with a localization accuracy of 15.5–16.9 mm when considering the highly clustered dipoles, as opposed to 30.4–32.5 mm when considering the scattered ones. Similarly, when comparing interictal ESI and MSI to the invasively defined IZ, we observed a localization error of 11.6–12.6 mm for clustered dipoles as opposed to 22.8–28 mm for scattered ones. If we consider a 15-mm distance as comparable to the average gyral width, we can infer that interictal ESI or MSI localization is able to reach a sublobar/gyral concordance with the invasively defined SOZ and IZ in our cohort (Kim et al., 2016). This finding demonstrates that interictal ESI and MSI can offer significant input in estimating the most epileptogenic areas even when the MRI findings do not help guide the surgical planning. This can expand the possibility of surgical treatment to patients who would not be otherwise considered surgical candidates.

Clustered dipoles provided a sensitivity and specificity to the SOZ of 69.1% and 61.5% for the LD-EEG ESI respectively. These values are comparable with previous studies in the field. Beniczky et al. (2013) performed ESI on ictal activity with LD-EEG reporting a sensitivity and specificity to the SOZ of 70% and 76% respectively. (Brodbeck et al., 2011) performed ESI with LD-EEG on interictal activity and reported sensitivity of 65% and specificity of 53% to the EZ respectively, after proof of resection considering patients with good surgical outcome (i.e. Engel I and II). Lower specificity values observed here and (Brodbeck et al., 2011), compared to Beniczky et al. (2013), are expectable since both studies localized interictal activity compared to ictal activity in Beniczky et al. (2013) that is more specific to the EZ. For the HD-EEG, clustered dipoles showed here a sensitivity and specificity to the SOZ of 65% and 60.7%, and to the IZ of 71.4% and 72.1% respectively. These values are also comparable with previous studies in the field. (Brodbeck et al., 2011) performed ESI with HD-EEG (128–256 channels) in a larger cohort of patients with DRE and reported a sensitivity of 84% and specificity of 88% for the EZ localization. For MSI, clustered dipoles provided a sensitivity and specificity to the SOZ of 74.4% and 49%, and to the IZ of 67.5% and 69.5% respectively. In a series of 1000 patients with DRE, Rampp et al (2019) showed that the sensitivity and specificity of MSI to complete MEG resection for an Engel 1 outcome was 66% and 83%. Yet, we should note that sensitivity and specificity values from different studies are not directly comparable due to the different methodological approaches and population groups under examination.

Our findings add to previous studies, which showed that the resection of dipole clusters is linked to a positive surgical outcome in patients with DRE (Almubarak et al., 2014, Ossenblok et al.,

2007, Vadera et al., 2013). Yet, previous literature has not been uniform regarding the definition of a cluster (Tanaka et al., 2018); researchers often use predefined criteria to label a dipole as either belonging to a cluster or not (Tamilia et al., 2019). Here, we estimated a quantitative metrics to assess the clustering level of each dipole and observed that it correlates with the epileptogenicity of the pointed area. Through this, we showed that the proposed clusterness measure can offer a useful quantitative index of epileptogenicity where the dipole is pointing at, without depending on an a-priori cluster definition. In addition, our study adds on the existing body of literature by demonstrating that both ESI and MSI benefit significantly from clustering analysis in children with DRE and inconclusive MRI. The value of dipole clustering has not been previously examined with LD-EEG and HD-EEG, particularly when performed on children with inconclusive MRI findings. Modalities with lower number of sensors (here LD-EEG and HD-EEG) were found to benefit more by our dipole clustering approach compared to modalities with higher number of sensors (e.g. MEG). In summary, our data suggest that the interpretation of interictal ESI and MSI is augmented by the use of quantitative metrics of clusterness in children with inconclusive MRIs, since this enhances the correlation between the non-invasive solutions and the gold standard defined through long-term invasive monitoring.

4.2. MSI and ESI are complementary for the SOZ and IZ localization

Although direct comparisons about the localization abilities of the different neuroimaging modalities (e.g. MEG and HD-EEG) cannot be drawn from this current study considering our small cohort, our findings imply a complementary role for ESI and MSI in the presurgical evaluation of children with DRE having normal MRI findings. No differences were observed between HD-EEG ESI and MSI for the IZ and SOZ localization. Moreover, there was no modality which consistently outperformed the others in the individual patient's level. Our findings are in line with Plummer and colleagues who evaluated HD-EEG and MEG without implementing any metrics of clusterness in a mixed population of children and adults with negative MRIs (Plummer et al., 2019) and showed the superiority of assessing ESI and MSI separately compared to each one alone or to their combined solutions. Here, LD-EEG ESI was outperformed by the HD-EEG ESI and MSI in the level of clustering but also provided useful information regarding the localization of the SOZ and IZ. Yet, if we look at each patient independently, as we do in clinical practice, this was not the case. At the individual level, for the SOZ estimation: MEG outperformed HD-EEG ($p < 0.05$) by ~15 mm in two cases (22.2%), HD-EEG outperformed MEG by ~7 mm in four cases (44.4%) ($p < 0.05$), while no difference was found in three cases (33.3%). Even though HD-EEG outperformed MEG in more cases, when MEG outperformed HD-EEG, it offered a larger improvement (Fig. 5a&c). HD-EEG outperformed LD-EEG by ~5 mm in two cases (22.2%) and no significant difference was found in seven cases (77.8%). MEG outperformed LD-EEG by ~55 mm in two cases (22.2%), while surprisingly LD-EEG outperformed MEG by ~12 mm in the same two cases where HD-EEG had also outperformed MEG. Similar results were found for the estimation of the IZ.

The complementary role of ESI and MSI in patients with inconclusive MRIs can be also deduced by their different sensitivity profiles and thus their ability to detect IEDs. MEG selectively detects tangential sources. On the other hand, EEG measures both radial and tangential activity, although the radial components dominate the EEG signals at the scalp. Therefore, MEG measures predominantly activity in the sulci of superficial cortex and is more prone to detect lateral neocortical IEDs, while both techniques seem to have comparable sensitivity profiles for epileptic activity arising from the mesial temporal lobe (Baumgartner, 2004). MEG and

EEG perform also differently depending on whether the IZ or SOZ is located within or outside the temporal lobe. HD-EEG have shown higher sensitivity in detecting IEDs for patients with temporal vs. extratemporal lobes epilepsy (sensitivity of 92% vs. 75%) (Brodbeck V et al., 2011). On the other hand, MEG provides higher diagnostic accuracy in extratemporal vs. temporal lobe epilepsy (sensitivity: 84% vs. 56%) (Rampp et al., 2019). In addition to the different sensitivity profiles, the differences observed in dipole clusterness among the three modalities (both inside and outside the SOZ and IZ) can be also attributed to the different number of sensors (here LD-EEG: 19 electrodes, HD-EEG: 72 electrodes, MEG: 306 sensors) and thus their different localization accuracy profiles (Song et al., 2015, Vrba et al., 2004).

4.3. Localization of mesial temporal and insular sources

The ability of MEG to identify deeper cortical sources of epilepsy, especially when originating from mesial temporal structures is questioned in multiple previous studies (Shigeto et al., 2002, Wennberg et al., 2011), but discredited by a recent study in patients with inconclusive MRI results (Plummer et al., 2019) and other studies in healthy adults (Papadelis et al., 2012). Here, MEG localized deep sources in 2 out of 3 patients who had the SOZ in the mesial temporal lobe with an accuracy of ≤ 20 mm (patients #2 and #3; MSI D_{SOZ} of clustered dipoles: 7.9 mm and 11 mm respectively) (Fig. 5a). MEG also successfully estimated the SOZ located to the insula in two patients (patient #5 and #10, MSI D_{SOZ} of clustered dipoles: 14.5 and 12.3 mm respectively). This is in line with (Heers et al., 2012) who highlighted the ability of MEG to localize spikes in patients with occult peri-insular epilepsy. The MEG ability to detect sources at the insular region is shown in patient #10 of our cohort, where semiology, non-invasive long-term EEG monitoring, interictal Single Photon Emission Computed Tomography (SPECT) and some subtle MRI findings were all pointing to the right frontal, frontotemporal and central regions. MEG was pointing to the right insula as the primary area generating the spikes. The invasive LTM with icEEG pointed to the right insula, the inferior frontal gyrus and the cingulate region and the hippocampus of the same side. Insular focus was ablated in all its width offering to the patient seizure freedom.

4.4. ESI and MSI correlate to the surgical outcome

To assess the relevance of ESI with LD-EEG and HD-EEG as well as MSI with MEG within the context of epilepsy surgery, it is of high importance to determine the link between the removal of the tissue pointed out by ESI or MSI and the post-surgical outcome. To this regard, we found that the proximity of both ESI and MSI to the resection was predictive of outcome: the D_{RES} was shorter and the percentage of resected dipoles was higher in the optimal compared to the suboptimal outcome group (Fig. 4; Fig. 5b&d). The clinical significance of this finding is supported by previous studies analyzing separately EEG and MEG, which reported that resection of the MSI or ESI solutions is important for the good post-surgical outcome in patients with inconclusive MRIs (Brodbeck et al., 2010, Fischer et al., 2005, RamachandranNair et al., 2007, Zhang et al., 2011). HD-EEG and MEG outperformed LD-EEG in patients with optimal surgical outcome who were proof of resection while no difference was found between ESI with HD-EEG and MSI with MEG (Fig. 4a). The significance of resecting MSI and ESI solutions is well depicted in patient #1 of our cohort who had no seizures captured with the icEEG. For this patient, the surgical resection included the areas pointed out by both the ESI and MSI, and ended up seizure free (Engel 1a). This case also highlights the importance of localizing the interictal activity non-invasively since icEEG does not always capture seizures.
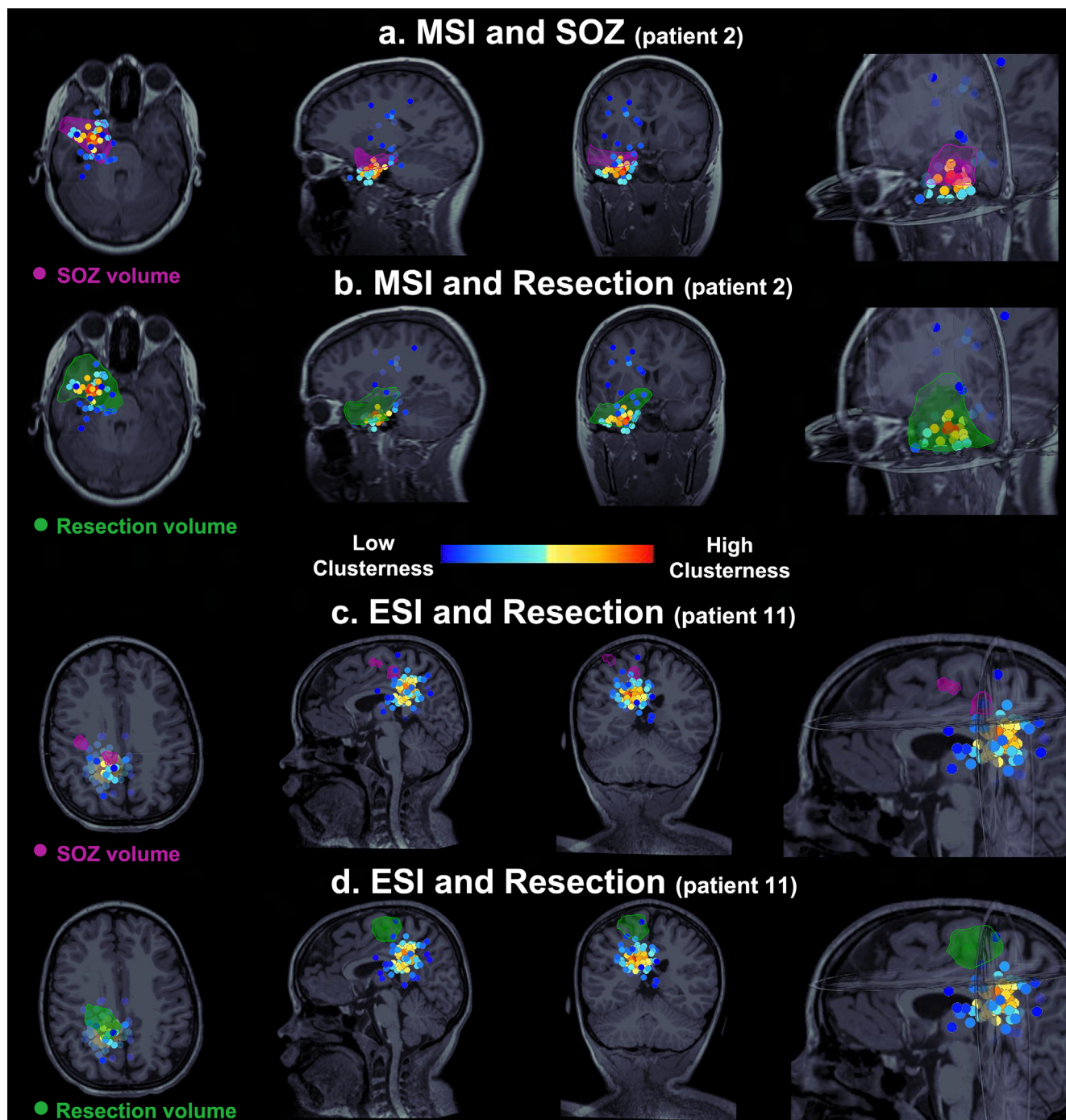
Fig. 5. Electric Source Imaging (ESI) and Magnetic Source Imaging (MSI) dipoles against ground truth given by Seizure Onset Zone (SOZ) and surgical resection. Patient with optimal outcome (a–b) and patient with suboptimal outcome (c–d). Each scenario shows the dipoles color coded based on their clusterness on the axial, sagittal, and coronal Magnetic Resonance Imaging (MRI) view. The SOZ is defined by the purple volume. The resection is defined by the green volume. (a–b) In the optimal outcome patient (patient #2), MSI dipoles with high clusterness show major overlapping with SOZ volume (a) and surgical resection (b). Dipoles with low clusterness (scattered) did not overlap with SOZ or resection. (c–d) In the suboptimal outcome patient (patient 11), ESI dipoles with high clusterness did not overlap with SOZ volume (c) and surgical resection (d). Only a few dipoles with low clusterness overlapped with SOZ and resection.

Our findings also suggest that not all ESI and MSI sources should be targeted during surgical planning. We found that the most epileptogenic dipoles are those characterized by high clustering. This is supported by our logistic regression analysis (Fig. 4b) showing that the proximity of clustered dipoles to the resection had a stronger correlation with the outcome compared to the proximity of all dipoles (both clustered and scattered) for both ESI and MSI. Finally, the percentage of resection of clustered dipoles was differ-

ent between patients with optimal and suboptimal outcome. This difference was not observed for the scattered dipoles.

4.5. Limitations

Our study has some limitations that should be taken into consideration while interpreting our results. The number of patients included in the study was limited due to our strict inclusion criteria.

Confirming this analysis on more patients would be an important validation of our findings in terms of generalizability: a multicenter, prospective study design would be an additional benefit of a future research done on this cohort. Due to the relatively small cohort, direct comparisons between the MEG and EEG regarding their localization abilities cannot be drawn from this study.

For statistical analysis, we chose not to average our measures per patient since we were interested in developing a clustering measure that can be applied to each dipole separately. Yet, this methodological approach may lead to findings which are susceptible to unbalanced numbers of dipoles between patients. In addition, there was a discrepancy between the number of channels for the LD-EEG (19-channels), HD-EEG (72-channels) and MEG (306 sensors): higher number of channels would probably improve the ESI results as postulated by previous studies (Hedrich et al., 2017, Lantz et al., 2003, Song et al., 2015). Finally, in order to perform ESI and MSI, we assumed that the detected epileptiform activity was generated by a single source which can be better localized using a dipole with a high GOF. Yet, this assumption has been recently challenged: ESI and MSI seems to localize the EZ more accurately at the earliest resolvable phase of IEDs rather than at the late peak-phase when the signal-to-noise ratios are maximal (Plummer et al., 2019). Although our analysis showed that on average the dipoles with the best GOF corresponded at earlier time points of the spike (several ms before the peak), we cannot guarantee that our ESI and MSI findings are not affected by propagation activity at some degree.

5. Conclusions

This study offers valuable insights into the presurgical evaluation of pediatric patients with epilepsy having normal MRIs or MRIs with subtle or non-focal findings. Non-invasive ESI with LD-EEG and HD-EEG as well as MSI with MEG can facilitate surgical planning and possibly limit the reliance on invasive monitoring, since they will allow estimating the invasively-defined SOZ and IZ, which are the main estimators of the EZ in surgical candidates. We observed that the ability to delineate the EZ and predict the surgical outcome is significantly improved when a quantitative measure of clusterness is used as an index of interpretation of interictal ESI and MSI. Advanced analysis of interictal ESI and MSI can augment the presurgical evaluation of children and young adults with normal, non-focal or subtly abnormal MRI, who may be regarded as ineligible for focal surgical resection with minimal or no functional loss.

Declaration of Competing Interest

The authors declare that they have no known competing financial interests or personal relationships that could have appeared to influence the work reported in this paper.

Acknowledgements

References

Abdallah C, Maillard LG, Rikir E, Jonas J, Thiriaux A, Gavaret M, et al. Localizing value of electrical source imaging: Frontal lobe, malformations of cortical development and negative MRI related epilepsies are the best candidates. Neuroimage Clin 2017;16:319–29.

Alhilani M, Tamilia E, Ricci L, Ricci L, Grant PE, Madsen JR, et al. Ictal and interictal source imaging on intracranial EEG predicts epilepsy surgery outcome in children with focal cortical dysplasia. Clin Neurophysiol 2020;131(3):734–43.

Almubarak S, Alexopoulos A, Von-Podewils F, Wang ZI, Kakisaka Y, Mosher JC, et al. The correlation of magnetoencephalography to intracranial EEG in localizing the epileptogenic zone: a study of the surgical resection outcome. Epilepsy Res 2014;108(9):1581–90.

Bagić A. Look back to leap forward: The emerging new role of magnetoencephalography (MEG) in nonlesional epilepsy. Clin Neurophysiol 2016;127(1):60–6.

Bast T, Oezkan O, Rona S, Stippich C, Seitz A, Rupp A, et al. EEG and MEG source analysis of single and averaged interictal spikes reveals intrinsic epileptogenicity in focal cortical dysplasia. Epilepsia 2004;45(6):621–31.

Baumgartner C. Controversies in clinical neurophysiology. MEG is superior to EEG in the localization of interictal epileptiform activity: Con. Clin Neurophysiol 2004;115(5):1010–20.

Benicky S, Lantz G, Rosenzweig I, Åkeson P, Pedersen B, Pinborg LH, et al. Source localization of rhythmic ictal EEG activity: a study of diagnostic accuracy following STARD criteria. Epilepsia 2013;54(10):1743–52.

Berkovic SF, McIntosh AM, Kalnins RM, Jackson GD, Fabinyi GCA, Brazenor GA, et al. Preoperative MRI predicts outcome of temporal lobectomy: an actuarial analysis. Neurology 1995;45(7):1358–63.

Brodbeck V V, Spinelli L, Lascano AM, Wissmeier M, Vargas MI, Vulliemoz S, et al. Electroencephalographic source imaging: a prospective study of 152 operated epileptic patients. Brain 2011;134(10):2887–97. https://doi.org/10.1093/brain/awr243.

Brodbeck V, Spinelli L, Lascano AM, Pollo C, Schaller K, Vargas MI, et al. Electrical source imaging for presurgical focus localization in epilepsy patients with normal MRI. Epilepsia 2010;51(4):583–91.

Chatrian GE. A glossary of terms most commonly used by clinical electroencephalographers. Electroencephalogr Clin Neurophysiol 1974;37:538–48.

Dale AM, Fischl B, Sereno MI. Cortical surface-based analysis I. Segmentation and surface reconstruction. Neuroimage 1999;9(2):179–94.

Diekmann V, Becker W, Jürgens R, Grözinger B, Kleiser B, Richter HP, et al. Localisation of epileptic foci with electric, magnetic and combined electromagnetic models. Electroencephalogr Clin Neurophysiol 1998;106(4):297–313.

Engel J, Van Ness PC, Rasmussen TB, Ojemann LM. Outcome with respect to epileptic seizures. In: Engel J, editor. Surgical treatment of epilepsies. 2nd ed. New York, NY: Raven Press; 1993. p. 609–21.

Fischer MJ, Scheler G, Stefan H. Utilization of magnetoencephalography results to obtain favourable outcomes in epilepsy surgery. Brain 2005;128:153–7.

Funke ME, Moore K, Orrison Jr WW, Lewine JD. The role of magnetoencephalography in "nonlesional" epilepsy. Epilepsia 2011;52(Suppl 4):10–4.

Gramfort A, Papadopoulo T, Olivi E, Clerc M. OpenMEEG: opensource software for quasistatic bioelectromagnetics. Biomed Eng Online 2010;9(1):45. https://doi.org/10.1186/1475-925X-9-45.

Hader WJ, Tellez-Zenteno J, Metcalfe A, Hernandez-Ronquillo L, Wiebe S, Kwon C-S, et al. Complications of epilepsy surgery: a systematic review of focal surgical resections and invasive EEG monitoring. Epilepsia 2013;54(5):840–7.

Hari R, Baillet S, Barnes G, Burgess R, Forss N, Gross J, et al. IFCN-endorsed practical guidelines for clinical magnetoencephalography (MEG). Clin Neurophysiol 2018;129(8):1720–47.

Hedrich T, Pellegrino G, Kobayashi E, Lina JM, Grova C. Comparison of the spatial resolution of source imaging techniques in high-density EEG and MEG. Neuroimage 2017;157:531–44.

Heers M, Rampp S, Stefan H, Urbach H, Elger CE, von Lehe M, et al. MEG-based identification of the epileptogenic zone in occult peri-insular epilepsy. Seizure 2012;21(2):128–33.

Jung J, Bouet R, Delpuech C, Ryvlin P, Isnard J, Guenot M, et al. The value of magnetoencephalography for seizure-onset zone localization in magnetic resonance imaging-negative partial epilepsy. Brain 2013;136(10):3176–86.

Kim D, Joo EY, Seo D-W, Kim M-Y, Lee Y-H, Kwon HC, et al. Accuracy of MEG in localizing irritative zone and seizure onset zone: Quantitative comparison between MEG and intracranial EEG. Epilepsy Res 2016;127:291–301.

Kwan P, Brodie MJ. Refractory epilepsy: a progressive, intractable but preventable condition?. Seizure 2002;11(2):77–84.

Lantz G, Grave de Peralta R, Spinelli L, Seeck M, Michel CM. Epileptic source localization with high density EEG: how many electrodes are needed?. Clin Neurophysiol 2003;114(1):63–9.

McGonigal A, Bartolomei F, Regis J, Guye M, Gavaret M, Fonseca A-T-D, et al. Stereoelectroencephalography in presurgical assessment of MRI-negative epilepsy. Brain 2007;130(12):3169–83.

Megevand P, Seeck M. Electroencephalography, magnetoencephalography and source localization: their value in epilepsy. Curr Opin Neurol 2018;31(2):176–83.

Minassian BA, Otsubo H, Weiss S, Elliott I, Rutka JT, Snead OC. Magnetoencephalographic localization in pediatric epilepsy surgery: comparison with invasive intracranial electroencephalography. Ann Neurol 1999;46(4):627–33.

Mohamed IS, Toffa DH, Robert M, Cossette P, Bérubé A-A, Saint-Hilaire J-M, et al. Utility of magnetic source imaging in nonlesional focal epilepsy: a prospective study. Neurosurg Focus 2020;48(4):E16. https://doi.org/10.3171/2020.1.FOCUS19877.

Murakami H, Wang ZI, Marashly A, Krishnan B, Prayson RA, Kakisaka Y, et al. Correlating magnetoencephalography to stereo-electroencephalography in patients undergoing epilepsy surgery. Brain 2016;139(11):2935–47.

Nagahama Y, Schmitt AJ, Nakagawa D, Vesole AS, Kamm J, Kovach CK, et al. Intracranial EEG for seizure focus localization: evolving techniques, outcomes,

complications, and utility of combining surface and depth electrodes. J Neurosurg 2018:1–13. https://doi.org/10.3171/2018.1.JNS171808.

Önal Ç, Otsubo H, Araki T, Chitoku S, Ochi A, Weiss S, et al. Complications of invasive subdural grid monitoring in children with epilepsy. J Neurosurg 2003;98 (5):1017–26.

Ono M, Kubik S, Abernathey CD. Atlas of the cerebral sulci. Stuttgart: Georg Thieme; .

Ossenblok P, de Munck JC, Colon A, Drolsbach W, Boon P. Magnetoencephalography is more successful for screening and localizing frontal lobe epilepsy than electroencephalography. Epilepsia 2007;48(11):2139–49.

Papadelis C, Leonardelli E, Staudt M, Braun C. Can magnetoencephalography track the afferent information flow along white matter thalamo-cortical fibers?. Neuroimage 2012;60(2):1092–105.

Papadelis C, Tamilia E, Stufflebeam S, Grant PE, Madsen JR, Pearl PL, et al. Interictal High Frequency Oscillations Detected with Simultaneous Magnetoencephalography and Electroencephalography as Biomarker of Pediatric Epilepsy. J Vis Exp 2016(118). https://doi.org/10.3791/54883.

Pellegrino G, Hedrich T, Chowdhury RA, Hall JA, Dubeau F, Lina J-M, et al. Clinical yield of magnetoencephalography distributed source imaging in epilepsy: A comparison with equivalent current dipole method. Hum Brain Mapp 2018;39 (1):218–31.

Plummer C, Vogrin SJ, Woods WP, Murphy MA, Cook MJ, Liley DTJ. Interictal and ictal source localization for epilepsy surgery using high-density EEG with MEG: a prospective long-term study. Brain 2019;142(4):932–51.

Prabhu S, Mahomed N. Imaging of intractable paediatric epilepsy. S Afr J Radiol 2015;19(2):1–10.

Radhakrishnan K, So EL, Silbert PL, Jack CR, Cascino GD, Sharbrough FW, et al. Predictors of outcome of anterior temporal lobectomy for intractable epilepsy: a multivariate study. Neurology 1998;51(2):465–71.

RamachandranNair R, Otsubo H, Shroff MM, Ochi A, Weiss SK, Rutka JT, et al. MEG predicts outcome following surgery for intractable epilepsy in children with normal or nonfocal MRI findings. Epilepsia 2007;48(1). https://doi.org/10.1111/epi.2007.48.issue-110.1111/j.1528-1167.2006.00901.x.

Rampp S, Stefan H, Wu X, Kaltenhäuser M, Maess B, Schmitt FC, et al. Magnetoencephalography for epileptic focus localization in a series of 1000 cases. Brain 2019;142(10):3059–71.

Semah F, Picot M-C, Adam C, Broglin D, Arzimanoglou A, Bazin B, et al. Is the underlying cause of epilepsy a major prognostic factor for recurrence?. Neurology 1998;51(5):1256–62.

Seo JH, Holland K, Rose D, Rozhkov L, Fujiwara H, Byars A, et al. Multimodality imaging in the surgical treatment of children with nonlesional epilepsy. Neurology 2011;76(1):41–8.

Shigeto H, Morioka T, Hisada K, Nishio S, Ishibashi H, Kira D-I, et al. Feasibility and limitations of magnetoencephalographic detection of epileptic discharges: simultaneous recording of magnetic fields and electrocorticography. Neurol Res 2002;24(6):531–6.

Siegel AM, Jobst BC, Thadani VM, Rhodes CH, Lewis PJ, Roberts DW, et al. Medically intractable, localization-related epilepsy with normal MRI: presurgical evaluation and surgical outcome in 43 patients. Epilepsia 2001;42(7):883–8.

Song J, Davey C, Poulsen C, Luu P, Turovets S, Anderson E, et al. EEG source localization: Sensor density and head surface coverage. J Neurosci Methods 2015;256:9–21.

Tadel F, Baillet S, Mosher JC, Pantazis D, Leahy RM. Brainstorm: a user-friendly application for MEG/EEG analysis. Comput Intell Neurosci 2011;2011:1–13.

Tamilia E, AlHilani M, Tanaka N, Tsuboyama M, Peters JM, Grant PE, et al. Assessing the localization accuracy and clinical utility of electric and magnetic source imaging in children with epilepsy. Clin Neurophysiol 2019;130(4):491–504.

Tamilia E, Dirodi M, Alhilani M, Grant PE, Madsen JR, Stufflebeam SM, et al. Scalp ripples as prognostic biomarkers of epileptogenicity in pediatric surgery. Ann Clin Transl Neurol 2020;7(3):329–42.

Tamilia E, Park E-H, Percivati S, Bolton J, Taffoni F, Peters JM, et al. Surgical resection of ripple onset predicts outcome in pediatric epilepsy. Ann Neurol 2018;84 (3):331–46.

Tanaka N, Papadelis C, Tamilia E, AlHilani M, Madsen JR, Pearl PL, et al. Magnetoencephalographic Spike Analysis in Patients With Focal Cortical Dysplasia: What Defines a "Dipole Cluster"?. Pediatr Neurol 2018;83:25–31.

Tonini C, Beghi E, Berg AT, Bogliun G, Giordano L, Newton RW, et al. Predictors of epilepsy surgery outcome: a meta-analysis. Epilepsy Res 2004;62(1):75–87.

Uusitalo MA, Ilmoniemi RJ. Signal-space projection method for separating MEG or EEG into components. Med Biol Eng Comput 1997;35(2):135–40.

Vadera S, Jehi L, Burgess RC, Shea K, Alexopoulos AV, Mosher J, et al. Correlation between magnetoencephalography-based "clusterectomy" and postoperative seizure freedom. Neurosurg Focus 2013;34(6):E9. https://doi.org/10.3171/2013.4.FOCUS1357.

Vrba J, Robinson SE, McCubbin J. How many channels are needed for MEG?. Neurol Clin Neurophysiol 2004;2004:99.

Wennberg R, Valiante T, Cheyne D. EEG and MEG in mesial temporal lobe epilepsy: where do the spikes really come from?. Clin Neurophysiol 2011;122 (7):1295–313.

Widjaja E, Shammas A, Vali R, Otsubo H, Ochi A, Snead OC, et al. FDG-PET and magnetoencephalography in presurgical workup of children with localization-related nonlesional epilepsy. Epilepsia 2013;54(4):691–9.

Wilenius J, Medvedovsky M, Gaily E, Metsähonkala L, Mäkelä JP, Paetau A, et al. Interictal MEG reveals focal cortical dysplasias: special focus on patients with no visible MRI lesions. Epilepsy Res 2013;105(3):337–48.

Zhang R, Wu T, Wang Y, Liu H, Zou Y, Liu W, et al. Interictal magnetoencephalographic findings related with surgical outcomes in lesional and nonlesional neocortical epilepsy. Seizure 2011;20(9):692–700.